PAIN Publish Ahead of Print
DOI: 10.1097/j.pain.0000000000002611

Anoctamin 1/TMEM16A in pruritoceptors is essential for Mas-related G protein receptor-dependent itch

Hyesu Kim[1,3,7], Hyungsup Kim[1,7], Hawon Cho[2], Byeongjun Lee[1], Huan-Jun Lu[1], Kyungmin Kim[1], Sooyoung Chung[1], Won-Sik Shim[4], Young Kee Shin[3], Xinzhong Dong[5], John N Wood[6], and Uhtaek Oh[1,3,*]

[1]Brain Science Institute, Korea Institute of Science and Technology (KIST), Seoul 02792, Korea.

[2]College of Pharmacy, Seoul National University, Seoul 08826, Korea

[3]Department of Molecular Medicine and Biopharmaceutical Sciences, Graduate School of Convergence Science and Technology, Seoul National University, Seoul 08826, Korea

[4]College of Pharmacy, Gachon University, Incheon 21936, Korea

[5]Solomon H. Snyder Department of Neuroscience, Johns Hopkins University School of Medicine, Baltimore, MD 21205, USA

[6]Molecular Nociception Group, Wolfson Institute for Biomedical Research, University College London, London WC1E 6BT, United Kingdom

[7]These authors contributed equally to this manuscript.

[*]To whom correspondence may be addressed. E-mail: utoh@kist.re.kr (L7 L7412, Brain Science Institute, Korea Institute of Science and Technology, 5 Hwarang-ro 14gil, Seongbuk-gu, Seoul 02792, Tel.: +82-2-958-7031, fax.: +82-2-958-7035)

ABSTRACT

Itch is an unpleasant sensation that evokes a desire to scratch. Pathologic conditions such

as allergy or atopic dermatitis produce severe itching sensation. Mas-related G protein receptors (Mrgprs) are receptors for many endogenous pruritogens. However, signaling pathways downstream to these receptors in dorsal root ganglion (DRG) neurons are not yet understood. We found that Anoctamin 1 (ANO1), a Ca^{2+}-activated chloride channel, is a transduction channel mediating Mrgprs-dependent itch signals. Genetic ablation of *Ano1* in DRG neurons displayed a significant reduction in scratching behaviors in response to acute and chronic Mrgprs-dependent itch models and the epidermal hyperplasia induced by dry skin. *In-vivo* Ca^{2+} imaging and electrophysiological recording revealed that chloroquine and other agonists of Mrgpr receptors excited DRG neurons via ANO1. More importantly, the overexpression of *Ano1* in DRG neurons of *Ano1*-deficient mice rescued the impaired itching observed in *Ano1*-deficient mice. These results demonstrate that ANO1 mediates the Mrgprs-dependent itch signaling in pruriceptors and provides clues to treating pathologic itch syndromes.

Keywords: Anoctamin 1; Pruriceptors; itch; Mrgprs; Bilirubin; Chloroquine

INTRODUCTION

Itch is a distinct sensation from pain, characterized by an unpleasant skin sensation. Acute itch works as a warning sign against transient harmful environments such as mosquito bites. Skin diseases such as atopic dermatitis, psoriasis, and cholestatic liver, kidney, and metabolic disorders cause chronic itch [2, 12, 14, 28]. Among diverse endogenous and exogenous pruritogens, histamine is the best-known itch-causing substance [28]. When tissues are inflamed or stimulated by allergens, histamine is released from mast cells [49]. Although antihistamines

are the current drug of choice for treating pruritus, many types of pruritic disorders, including atopic dermatitis, are poorly treated with antihistamines [21]. Thus, histamine-independent mechanisms appear to be involved in chronic itch.

Mas-related G protein-coupled receptors (Mrgprs), a large class of receptors expressed solely in dorsal root ganglion (DRG) neurons, are now known to transduce histamine-independent itch [26, 27, 51]. Among the Mrgprs family in mice, MrgprA3 is stimulated by chloroquine (CQ), an anti-malarial drug whose complication is a severe itch sensation [57]. BAM8-22, an endogenous bovine adrenal medulla peptide, evokes itch via activation of MrgprC11 [51]. Ser-Leu-Ile-Gly-Arg-Leu (SLIGRL) is an agonist of protease-activated receptor 2 (PAR2) that induces neuronal excitation and scratching behaviors in mice [52]. SLIGRL is now known to cause itch through MrgprC11 rather than PAR2 because scratching responses by SLIGRL was attenuated in *MrgprC11*-deficient mice rather than PAR2-null mice [27]. TRPA1 was reported as a downstream channel to MrgprA3- and MrgprC11-induced itch mainly because BAM8-22 and CQ-evoked itch and the excitation of itch fibers require TRPA1 [57]. However, this mechanism is challenged because the excitation of cutaneous c-fibers by CQ or BAM8-22 in the skin-nerve preparation is not reduced by the application of a TRPA1 blocker or in *Trpa1*-deficient mice [42]. On the other hand, the CQ-induced action potential discharge and scratching behaviors were significantly decreased by an ANO1 specific blocker, suggesting a role of ANO1 in itch sensation [42]. Therefore, the signaling pathway underlying histamine-independent itch is still unclear.

Anoctamin 1 (ANO1, also known as TMEM16A) is a Ca^{2+}-activated chloride channel mediating numerous physiological functions [5, 46, 60]. ANO1 regulates mucus secretion in airway epithelia, fluid secretion in intestines and salivary glands, and affects vascular contractility [16, 40]. ANO1 promotes tumorigenesis in numerous cancer cells [4, 30] and induces testosterone-dependent benign prostate hyperplasia [6]. ANO1 regulates the radial glial

function in the developing brain [13]. More importantly, ANO1 is expressed in a subset of small-diameter DRG neurons, thereby mediating thermal pain as a heat sensor [8]. Nociceptive behaviors to heat, inflammation, or neuropathic conditions are substantially reduced by ANO1 blockers or genetic deletion of *Ano1* [8, 17, 23, 25]. Because ANO1 is expressed in small-sized DRG neurons, which are primarily associated with itch [8, 28, 45], it is tempting to assume that ANO1 may mediate itch. Using mice with DRG-specific genetic ablation of *Ano1*, this study was aimed to determine whether ANO1 mediates Mrgprs-related itch. As a result, *Ano1*-deficient mice showed a substantial reduction in scratching behaviors in response to Mrgprs-related pruritogens or various chronic itch models.

RESULTS

Genetic ablation of Ano1 in DRG neurons reduces Mrgprs-related scratching

To determine whether ANO1 is involved in itch sensation, we tested if $Adv^{CRE}Ano1^{fl/fl}$ mice, the DRG neuron-specific conditional knock-out (cKO) mice that lacked *Ano1* in DRG neurons [8], showed reduced scratching behaviors in response to various pruritogens. We first tested if the genetic ablation of *Ano1* affects Mrgprs-dependent itch. Because CQ, an anti-malarial drug, and SLIGRL are known to cause non-histaminergic, Mrgprs-dependent itch[2, 26, 28], CQ (200 μg/100 μl) and SLIGRL (65 μg/100 μl) were injected into the neck of littermate control (CTL; $Ano1^{fl/fl}$) and cKO mice. When CQ and SLIGRL were injected, CTL mice scratched the neck skin vigorously with the hind limbs. In contrast, cKO mice scratched significantly less than CTL mice in response to the CQ and SLIGRL injections (Fig. 1A). Also, CQ-induced scratching behaviors were significantly reduced when CQ was co-injected with an ANO1 inhibitor, *N*-((4-methoxy)-2-naphthyl)-5-nitroanthranilic acid (MONNA, 35

μg/100 μl) (Fig. 1B) [38].

When histamine (200 μg/100 μl) and endothelin-1 (125 ng/100 μl), which are Mrgprs-independent pruritogens [15, 28], were injected into the neck of CTL mice, these pruritogens evoked scratches comparable to those observed by others [15]. *Ano1* cKO mice's scratching behaviors in response to these Mrgprs-independent pruritogens did not differ from those of CTL mice (Fig. 1C). In addition, when serotonin (5-HT, 20 μg/100 μl), another pruritogen released from mast cells [36, 59], was injected, the two genotype mice scratched the neck with comparable frequencies (Fig. 1C).

Genetic ablation of Ano1 reduces scratching in Mrgprs-dependent chronic itch models

Cholestasis is a common disease characterized by a reduced bile acid flow [12]. One of its complications is pruritus [12]. The systemic increase in bile acids and other endogenous substances causes pruritus [12]. Recently, molecular and neuronal mechanisms underlying cholestatic pruritus have been identified. Bilirubin in the skin is now known to evoke itching via MrgprX4 or MrgprA1 in humans or mice, respectively [32]. Therefore, we tested whether ANO1 contributes to cholestatic pruritus. The subcutaneous injection of bilirubin (60 μg/ 50 μl) to the nape of CTL mice elicited scratching. In contrast, the cKO mice scratched significantly less than the CTL mice in response to the bilirubin injection (Fig. 1D).

Dry skin causes itch [35], which is now classified as non-histaminergic itch because the dry skin-evoked scratching is not affected by antihistamine treatment [1, 35, 58]. Moreover, MrgprA3 is known to mediate the dry skin-evoked itching [11, 63]. Therefore, we tested whether the genetic ablation of *Ano1* affects dry skin-induced scratching. We generated the dry skin model after a gentle wash on cheeks with the acetone and ether mixture followed by a wash with water (AEW) [1, 35, 63]. The repeated applications of AEW for 3 or 5 days to the cheek caused scratchings in CTL mice compared to the water-treated mice (Fig. 1E). In contrast, the

cKO mice scratched significantly less than CTL mice after 3 and 5 days of the AEW treatment (Fig. 1E).

The repeated application of AEW is known to cause epidermal hyperplasia [35, 58]. Indeed, the repeated application of AEW to the skin caused prominent epidermal hyperplasia in CTL mice compared to the epidermis of the water-treated skin (Fig. 2A). In contrast, the repeated application of AEW also caused epidermal hyperplasia in cKO mice but with much less extent than in CTL mice (Figs. 2B and C). Therefore, these results suggest that ANO1 mediates dry skin-induced itch, a MrgprA3-dependent chronic itch model [11, 63].

Psoriasis is a chronic skin disease characterized by thickened stratum corneum (hyperkeratosis) that causes severe pruritus [62]. Repeated topical application of imiquimod, an agonist of Toll-like receptor 7 in DRG neurons, is a model for psoriasis-like itch in mice and humans [19, 29, 43]. We, therefore, determined whether ANO1 involves in psoriatic itch. When imiquimod cream was applied to mice's necks every day for 7 days, the CTL mice elicited pronounced spontaneous scratches from as early as 3 days after the application. The spontaneous scratches of cKO mice were comparable to those of the CTL mice in 3, 5, and 7 days of the imiquimod application (Fig. S1, available as supplemental digital content at http://links.lww.com/PAIN/B585). Thus, these results strongly suggest that ANO1 mediates non-histaminergic, Mrgprs-dependent itch

ANO1 expression in MrgprA3 positive DRG neurons

Because ANO1 is expressed mainly in small DRG neurons [8], we thus examined whether it is also expressed in itch sensory neurons. Because MrgprA3 is considered a marker for itch fibers [11, 57], we determined the co-localization of ANO1 and MrgprA3 in *MrgprA3*$^{GFP\text{-}Cre}$ transgenic mice [11]. As shown in Fig. 3A, ANO1 is expressed in many DRG neurons, where GFP-positive neurons were also co-localized. Among 1,432 ANO1-positive neurons, 403

(28.1%) were also positive for MrgprA3 (Fig. 3B). Importantly, 93.9% of MrgprA3 positive neurons were also positive to ANO1 (Fig. 3B). These results suggest that a large proportion of MrgprA3-positive DRG neurons overlaps with ANO1-positive neurons. In contrast, the proportion of histamine H1 receptor (H1R)-positive neurons was low in ANO1-positive DRG neurons (Fig. 3C). Among 993 ANO1-positive neurons, only 96 neurons (9.7%) were H1R-positive (Fig. 3D). Similarly, 31.5% of H1R-positive neurons (305 neurons) were ANO1 positive (96 neurons) (Fig. 3D). These results are consistent with the lack of phenotype of Ano1-cKO mice to histamine (Fig. 1C).

ANO1 mediates CQ- and SLIGRL-induced excitation of DRG neurons

Although ANO1 is a chloride ion channel, it was proven to depolarize DRG neurons when activated [8]. Therefore, we determined whether ANO1 mediates the CQ or SLIGRL-induced neuronal excitation of DRG neurons. We recorded membrane potentials of relatively small-diameter DRG neurons (<30 μm) isolated from CTL or *Ano1* cKO mice. The 1 mM CQ application caused depolarization with multiple action potentials in cultured DRG neurons from CTL mice (Fig. 4A). Some neurons showed firing with depolarization, while some other neurons showed depolarization without firing. The CQ application triggered action potential firings in 22 out of 107 DRG neurons (20.6%) isolated from CTL mice. In contrast, the CQ application failed to evoke action potential firings in the majority of DRG neurons obtained from *Ano1* cKO mice (Fig. 4A). Only 1 out of 35 DRG neurons (2.9%) isolated from *Ano1* cKO mice responded to the CQ. In addition, the application of an ANO1 inhibitor MONNA (10 μM) also inhibited these action potentials evoked by CQ in DRG neurons from CTL mice (Fig. 4B). The CQ application depolarized the neurons with 29.7 ± 4.8 mV (n = 7), which was significantly reduced to 13.9 ± 4.1 mV (n = 7) by MONNA (10 μM) (Fig. S2A, available as supplemental digital content at http://links.lww.com/PAIN/B585).

In addition, CQ (1 mM) evoked small but robust inward currents in DRG neurons of CTL mice. The CQ-induced inward currents were reduced by 10 μM MONNA (Fig. S2B, available as supplemental digital content at http://links.lww.com/PAIN/B585). Thus, these results indicate that ANO1 mediates the CQ-induced excitation of DRG neurons.

Similarly, the application of 1 mM SLIGRL also caused a barrage of action potentials when applied to DRG neurons from CTL mice (Fig. 4C). The proportion of DRG neurons of CTL mice responding with action potential firing to the SLIGRL application was 35.4% (23 out of 65 DRG neurons) (Fig. 4C). In contrast, only 10.5% of DRG neurons (4 out of 38) from *Ano1* cKO mice responded to the SLIGRL application (Fig. 4C). In addition, 10 μM MONNA completely blocked the SLIGRL-induced excitation of DRG neurons (Fig. 4D). These results suggest that ANO1 also mediates the SLIGRL-induced excitation in DRG neurons.

Pharmacological block of ANO1 inhibits CQ-evoked DRG neuron activity in vivo

To determine if CQ activates a subset of DRG neurons via ANO1 *in vivo*, GCaMP-based optical Ca^{2+} imaging was attempted on DRG neurons in anesthetized mice. CaMKIIa-based GCaMP6f-expressing ($CaMKIIa^{CRE}GCaMP6f^{fl/+}$) male mice were deeply anesthetized. Their L4 DRGs were exposed and placed under a two-photon microscope to measure the activities of DRG neurons *in vivo* [7, 20]. Representative images of neurons that showed fluorescence responses before (left) and after (right) intraplantar CQ injection are indicated by arrowheads (Fig. 5A). Applying KCl (250 mM) directly on the DRG neurons evoked robust fluorescence signals of GCaMP6f-expressing DRG neurons (Fig. 5B). CQ (400 μg/10 μl) was injected into the ipsilateral hind paw (at time 0 min, arrow) (Fig. 5C). The intraplantar injection of CQ evoked spiking or prolonged fluorescence signals (Figs. 5A and C). When MONNA was coinjected with CQ, the fluorescent activity was strikingly reduced (Figs. 5D and E).

Background fluorescence signals with $F/F_0 < 1.0$ or with a slow and gradual increase were excluded as non-responders. In addition, the proportion of responding neurons to the CQ injection was significantly reduced by the MONNA coinjection: 60 out of 425 neurons (14%) were active in response to CQ injection alone, whereas only 56 out of 699 (8%) neurons were active in response to the CQ+MONNA injection (Fig. 5F). We assessed the total number of functional neurons after counting fluorescent neurons in response to the direct application of 250 mM KCl to DRGs (Fig. 5B).

Stimulation of MrgprA1, A3, or MrgprC11 activates ANO1

MrgprA3 is a G-protein coupled receptor essential for the CQ-induced signaling in sensory neurons and the CQ-evoked itch [57]. Therefore, we determined whether the stimulation of MrgprA3 could activate ANO1 in a heterologous system. Mouse *Mrgpra*3 and *Ano1* were transfected to human embryonic kidney 293T (HEK) cells. To measure the Cl^- currents, bath and pipette solutions contained 140 mM NMDG-Cl to make Cl^- as a sole charge carrier. As shown in Figure 6A, the application of 500 μM CQ induced robust Cl^- currents in HEK cells transfected with *Mrgpra3* and *Ano1* at the holding potential of -60 mV. However, the CQ failed to evoke currents in HEK293T cells transfected with *Mrgpra3* or *Ano1* alone (Fig. 6A and B).

Similarly, because MrgprC11 is known to be a receptor for SLIGRL for itch sensation [27], we also tested whether ANO1 is a downstream effector for MrgprC11. Because SLIGRL evoked currents in native HEK293T cells, presumably due to the PAR2 signaling pathway [18], Chinese hamster ovarian K-1 (CHO) cells were used instead for the reconstitution study. The application of 1 mM SLIGRL evoked robust Cl^- currents in CHO cells transfected with *Mrgprc11* and *Ano1,* whereas the SLIGRL application failed to evoke currents in CHO cells transfected with *Mrgprc11* or *Ano1* alone (Figs. 6C and D).

Bilirubin is known to stimulate mouse MrgprA1 and human MrgprX4 [32, 33]. Thus, ANO1 should be activated by the bilirubin-stimulated MrgprA1 if ANO1 is the downstream transduction channel for MrgprA1. Indeed, the application of 50 μM bilirubin to HEK293T cells transfected with *Mrgpra1* and *Ano1* evoked strong currents. However, the bilirubin failed to produce currents in HEK293T cells transfected with *Mrgpra1* or *Ano1* alone (Figs. 6E and F). Thus, these results suggest that ANO1 is a downstream effector to MrgprA1, A3, and C11.

Mutants of yellow fluorescence protein (YFP) have been used to measure Cl^- channel activity as they have the potential to exhibit strong fluorescence by binding with chloride, whereas it loses fluorescence with iodide binding [39, 56]. Therefore, after adding an iodide-containing solution to a chloride-containing extracellular solution, we measured the quenched fluorescence as an indicator of ANO1 activity. YFP-H148Q/I152L/F46L, a widely-used halide sensor, was used [37]. Thus, the fluorescence intensity of HEK293T cells transfected with *MrgprA3*, *Ano1*, and *Yfp-H148Q/I152L/F46L* was measured. Upon 1 mM CQ treatment, the fluorescence showed robust extinction in HEK293T cells expressing both *MrgprA3* and *Ano1* (Fig. 7A). However, when *MrgprA3* or *Ano1* alone was transfected, the fluorescence failed to show an abrupt decay. Likewise, the YFP fluorescence showed robust extinction upon 100 μM SLIGRL treatment to CHO cells transfected with *MrgprC11* and *Ano1*. However, when *MrgprC11* or *Ano1* alone was transfected, the fluorescence failed to decay (Fig. 7B). Similarly, the application of 100 μM bilirubin caused a rapid quenching of the YFP fluorescence in HEK293T cells expressing *MrgprA1* and *Ano1*, whereas it failed to show a quenching fluorescence of YFP in HEK293T cells transfected with *MrgprA1* or *Ano1* alone (Fig. 7C). Thus these results further support the notion that stimulation of MrgprA3, MrgprC11, and MrgprA1 with their respective ligands activates ANO1.

PLC signaling mediates the ANO1/MrgprA3 or MrgprC11 pathway

ANO1 is activated by intracellular Ca^{2+} via the phospholipase C (PLC)/IP_3 pathway [60]. Therefore, we determined whether the PLC signaling is required for the SLIGRL-evoked excitation of DRG neurons. We applied 1 mM SLIGRL twice to DRG neurons in a 5-min interval to see the PLC inhibitor's effect on the SLIGRL-induced neuronal excitation. The application of 1 μM U73122, a PLC inhibitor, completely blocked the SLIGRL-evoked excitation of DRG neurons (Figs. S3A and B, available as supplemental digital content at http://links.lww.com/PAIN/B585).

Similarly, we also determined the involvement of PLC in the MrgprA3/ANO1 pathway in the reconstitution study. CQ induces inward currents with mild desensitization in HEK293T cells transfected with *Mrgpra3* and *Ano1* (Figs. S3C and D, available as supplemental digital content at http://links.lww.com/PAIN/B585). The second CQ application evoked about 49.7 ± 17.2% (n = 5) of the 1st current amplitudes. However, the application of 1 μM U73122 along with CQ inhibited the CQ-induced currents to 8.3 ± 4.1% of the 1st current amplitudes. Thus, these results indicate that PLC mediates the MrgprA3/ANO1 and MrgprC11/ANO1 signaling pathways.

Overexpression of Ano1 in the DRGs of Ano1 cKO mice rescues the CQ-induced itching

To confirm the role of ANO1 in mediating the Mrgprs-dependent itch, we systemically overexpressed *Ano1* in the *Ano1* cKO mice to see if the impaired CQ-induced itching is rescued. We injected AAV2-hSyn-mCherry (mock virus) or AAV2-hSyn-Ano1-mCherry (rescue virus) into the temporal vein of newborn CTL and cKO mice [10]. As shown in Figure 8A, mCherry, the reporter gene, was well expressed in DRG neurons of virus-injected mice, suggesting the successful targeting of the virii to DRG neurons. The subcutaneous injection

of CQ (400 μg/100 μl) into the neck caused robust scratching in the mock virus injected CTL mice, whereas it caused a significantly less frequent scratching in the mock virus injected cKO mice (Fig. 8B). In contrast, the subcutaneous CQ injection evoked almost identical numbers of scratching in both the CTL and cKO group when the rescue virus was injected, suggesting that the reduction in CQ-induced itching observed in cKO mice was rescued by the overexpression of *Ano1* in the DRGs of cKO mice (Fig. 8B).

DISCUSSION

Itch is a distressful sensation for scratching the skin to avoid harmful stimuli. Severe and lasting itch often deliberates the patient's quality of life, disturbing sleep and mood [61]. Harmful environmental stimuli such as mosquito-bite evoke acute itch that does not last long. Meanwhile, chronic itch is defined as a prolonged itch condition longer than six weeks [61]. Chronic itch accompanies severe pathological conditions such as atopic dermatitis, psoriasis, and allergies. These skin abnormalities cause an unbearable itch that brings intense scratching. These scratches aggravate dermatitis conditions, which leads to the vicious itch-scratch-itch cycle. The current treatment for the itch is anti-histamines. However, the pharmacological effects of antihistamines on chronic itch are minimal [61]. Therefore, therapeutic options for the histamine-independent itch become an essential issue for itch treatment.

The present study identified the role of ANO1 in mediating Mrgprs-dependent itch because scratching evoked by Mrgprs-dependent pruritogens was significantly reduced in *Ano1*-deficient mice. In addition, a portion of spontaneous and persistent itch induced by dry skin conditions was also reduced. Applications of CQ, SLIGRL, and bilirubin activate ANO1

in sensory neurons via MrgprA3, MrgprC11, and MrgprA1, respectively. More importantly, *in-vivo* Ca^{2+} imaging of DRG neurons revealed CQ-induced neural activity's antagonism by an ANO1 blocker. Thus, ANO1 appears to contribute to transmitting the Mrgprs-dependent itch in the periphery.

Itch signaling pathway in pruriceptors

Many ion channels with a role in nociception also act as downstream effectors in itch signaling pathway [2, 28]. TRPV1, a key channel for nociception, is also known to mediate histamine-induced itch [49]. A subset of DRG neurons were both activated by capsaicin and histamine. In addition, histamine-evoked Ca^{2+} signals in DRG neurons, as well as itching, are not observed in *Trpv1*$^{-/-}$ mice [50]. Activity-dependent silencing of TRPV1-expressing neurons with a pore-permeable Na^{+} channel blocker, QX-314, silences histamine-evoked scratching [41]. In addition, a downstream channel for MrgprA3 and C11 was reported to be TRPA1. A subset of DRG neurons that respond to mustard oil, an agonist for TRPA1, also respond to CQ and BAM8-22 [57]. The numbers of DRG neurons responding to these pruritogens are significantly reduced in *Trpa1*$^{-/-}$ mice. In addition, *Trpa1*$^{-/-}$ mice show less scratching after subcutaneous injection of CQ and BAM8-22. TRPA1 also appears to mediate the dry skin-induced chronic itch [58]. However, the role of TRPA1 in mediating the histamine-insensitive itch is challenged because CQ-evoked itch and neural excitation of DRG neurons from *Trpa1*$^{-/-}$ mice are comparable to those of the WT mice [42]. In the present study, we showed that ANO1 contributes to itching via the downstream signal to the Mrgprs. ANO1 is a Cl^{-} channel activated by intracellular Ca^{2+} and voltage [60]. Many physiological ligands such as ATP, acetylcholine, histamine, and endothelin-1 can activate ANO1 via PLCβ stimulated by their respective receptors [60]. Bradykinin, which induces inflammatory pain, also opens ANO1 through PLC signaling by tethering of ANO1 and IP_3R [17, 25]. Therefore, it is not surprising to

know that CQ, SLIGRL, and bilirubin open ANO1 via respective Mrgpr receptors in DRG neurons.

Common transducers for pain and itch in DRG neurons

Itch and pain are distinct unpleasant sensations, but they are closely related. For example, pain and itch are antagonistic. Scratching the skin suppresses the itch sensation [44]. The close relationship between pain and itch partly comes from the fact that many itch fibers overlap with nociceptors [22]. In addition, spinal neurons activated by pruritogens are also activated by painful stimuli [15, 49, 57]. Therefore, the neural conduction pathway for the itch is considered a part of the pain pathway. According to this 'Intensity theory' model, when nociceptors in the skin are stimulated intensely, pain sensation is obtained, whereas when the same nerves are lightly activated, then itch sensation ensues [3, 9]. However, the discovery of itch-specific sensory neurons, interneurons, and projection neurons in the spinal cord supports the 'labeled line' theory [9]. Mice deficient of MrgprA3-positive DRG neurons exhibited decreased scratching behaviors, but not pain behaviors [11]. Gastrin-releasing peptide(GRP)- and natriuretic polypeptide B-positive neurons in the spinal cord evoke itch but not pain responses supporting the labeled line theory [34, 54]. However, these two theories are not mutually exclusive. Sun and colleagues proposed a leaky gate model theory [53], where GRP-positive interneurons in the dorsal horn of the spinal cord receive both pain and itch sensory inputs and evoke pain and itch when activated. Recently, even stimulation of MrgprA3-positive c-fibers evokes either itch or pain-like behaviors depending on the metabotropic or ionotropic stimulation, suggesting that differential stimulation of the same neuronal population results in itch or pain [48].

In this context, it is worth noting that some key molecules in DRG neurons mediate itch and pain. For example, TRPV1 and TRPA1, transducer channels for nociception, are also

known to mediate itch [50, 57, 58]. Similarly, ANO1 is thought to be a heat sensor responsible for thermal pain and is now considered to mediate itch [8, 23, 25]. The majority of ANO1-positive neurons were Mrgpr-negative (Fig. 3). Therefore, these ANO1-positive, Mrgpr-negative DRG neurons may participate in pain signaling. Ca^{2+} influx through TRPV1 activates ANO1 [55]. In addition, more complex mechanisms for the functional coupling between TRPV1 and ANO1 were suggested: Ca^{2+} influx through TRPV1 activates Ca^{2+}-sensitive PLC, which releases IP_3 and induces Ca^{2+} release from the ER, thereby activating ANO1 [31, 47]. This synergistic action of TRPV1 and ANO1 induces a pain-enhancing effect. Thus, the dual roles of these transducer channels for pain and itch signals in a subset of DRG neurons may further support the idea that pain and itch share common molecular and neural components in their conduction pathways.

In summary, current study identified that ANO1 mediates Mrgpr-dependent itch. Because chronic itch reduces the quality of life, molecular mechanisms underlying Mrgpr-dependent itch in the present study would provide a clue to cure some types of chronic itch. Therefore, ANO1 could be a new therapeutic target for itch treatment.

METHODS

Generation of Ano1 cKO mice

The generation of *Ano1* cKO mice was described previously [8]. Briefly, the *Ano1* targeting construct was built by conventional cloning. In the construct, exon 8 was flanked by *loxP* sites followed by an FRT-flanked neo cassette. The targeting vector was linearized and inserted into embryonic stem cells (Sv129/R1) with electroporation. Neomycin-resistant cells

were selected with geneticin (G418). The positive clones were confirmed by Southern blot analysis using a probe after digestion with *Sacl.* Cloned embryonic stem cells were injected to blastocysts of C57BL/6 mice, which produced a large number of chimeric mice. To generate heterozygous mice carrying one floxed allele ($Ano1^{fl/+}$), these chimeric mice were bred with C57BL/6 mice. The neo cassette was removed by crossing $Ano1^{fl/+}$ to Deleter-FlpE mice (Jackson Laboratory, stock #003800). The $Ano1^{fl/+}$ mice without neo-cassette were then crossed with Adv^{CRE} to produce $Adv^{CRE}Ano1^{fl/+}$ mice. The $Adv^{CRE}Ano1^{fl/+}$ mice were crossed with $Ano1^{fl/+}$ mice to generate $Adv^{CRE}Ano^{fl/fl}$ (cKO) mice in DRG neurons. $Ano1^{fl/fl}$ mice without Cre-expression were used for CTL mice.

Behavioral tests

Animal care: All experiments were performed on 7-15 weeks old mice. These animals were housed in a controlled environment, on a 12-h light/dark cycle, with free access to food and water. Animal experiments were carried out in accord with the Ethical Guidelines of the International Association for the Study of Pain. All animal experiments were approved by the Institute of Laboratory Animal Resources of the Korea Institute of Science and Technology.

Pruritic compound preparation: Pruritogens such as CQ (200 or 400 μg/100 μl, Sigma), SLIGRL (65 μg/100 μl, Tocris), histamine (200 μg/100 μl, Sigma), serotonin (5-HT, 20 μg/100 μl, Sigma), endothelin-1 (ET-1, 125 ng /100 μl, Sigma) were dissolved in the Ringer solution. MONNA (35 μg/100 μl, Tocris) was dissolved in DMSO and diluted with Ringer solution before use. Bilirubin (60 μg/50 μl, Frontier Scientific) was freshly prepared before the behavior test in 0.01N NaOH and then maintained in the dark. For whole cell current recording test, bilirubin was dissolved in DMSO and then diluted into bath solution with final DMSO concentration < 0.5%.

Pruritogen-induced scratching test: Both male and female mice were used for behavior tests. Mice were anesthetized by intraperitoneal injection of a mixture of Zoletil 50

and Rompun at a ratio of 2:1. When mice were anesthetized, they were shaved at the dorsal neck or cheeks for the application of pruritogens. Mice were allowed to acclimate to a chamber for 30 min before behavioral tests, and then pruritogens were injected into the shaved nape of the neck of mice. One scratch was defined as a lifting of hind limbs near the nape or cheeks and a replacing of the hind limb back to the floor. After injection, mice were placed back in the chamber and recorded by a video camera for 30 min. All behavioral tests were conducted blinded to genotype or treatment.

Dry skin-evoked scratching test: To generate dry skin-induced itch behaviors in the cheeks of mice, both cheeks were shaved, and a mixture of acetone and ether (1:1) were treated lightly with a cotton swab at shaved cheeks of mice for 15 s, followed by wash with water for 30 seconds. This treatment was carried out three times a day for 5 days. Scratching behaviors of the acetone, ether, and water-treated mice were recorded by a video camera for 30 min.

Imiquimod-induced scratching test: Mice older than 2 months were used. After anesthesia, the nape of the neck of mice were shaved, and 42 mg of Aldara cream® (DongA-ST, 5% Imiquimod) was applied to the nape of the neck of mice for 7 days. At 3rd, 5th, 7th day of the experiment, mice were allowed to acclimate to a chamber for a 30 min after 4 hours of the application, and then mice were recorded by a video camera for 1 hour. The number of scratching bouts were counted.

Viral injection: Overexpression of *Ano1* in the *Ano1* cKO mice was obtained with AAV virus infection. AAV2-hSyn-mCherry or AAV2-hSyn-Ano1-mCherry was injected into the temporal vein of the newborn (P1) cKO and CTL mice with a 31-gauge insulin syringe [10]. Ten weeks-old mice were tested for CQ-evoked scratching. After the scratching test, mice were sacrificed for confirming the mCherry expression.

Immunofluorescent staining

Immunofluorescent staining of DRGs for ANO1, MrgprA3 and H1R was performed as previously described [11]. Briefly, dissected mouse DRGs from wild type and *MrgprA3*$^{GFP\text{-}Cre}$ mice were sectioned on a cryostat at 10 μm and fixed in methanol. Sections were washed, incubated with blocking buffer (4% bovine serum albumin in phosphate-buffered saline with TWEEN 20) for 30 min. For ANO1 and MrgprA3, sections were incubated with rabbit ANO1 monoclonal antibody raised against mouse ANO1 (Abcam, Cambridge, MA) (diluted 1:50), rabbit anti-GFP (diluted 1:500, in blocking solution, Chemicon Intl. Inc., Temecula, CA) for overnight at 4^{o}C. Samples were then washed and incubated with secondary antibody Alexa Fluor 594-conjugated donkey anti-rabbit (diluted 1:400, Molecular Probe) for ANO1 and FITC-conjugated Donkey anti-guinea pig (diluted 1:400, Chemicon Intl. Inc.) at room temperature for 1 hour. Labeled DRG sections were imaged using the Leica TCS confocal system (Leica Microsystems, Heidelberg, Mannheim, Germany). For ANO1 and H1R, sections were incubated with rabbit ANO1 monoclonal antibody raised against mouse ANO1 (Abfrontier, diluted 1:200), mouse H1R monoclonal antibody raised against mouse H1R (Santa Cruz, diluted 1:150) for overnight at 4^{o}C. Samples were then washed and incubated with secondary antibody Alexa Fluor 488-conjugated chicken anti-rabbit (diluted 1:300) and Alexa Fluor 555-conjugated donkey anti-mouse (diluted 1:300) at room temperature for 1 hour. Labeled DRG sections were imgaed using Zeiss Confocal System (Carl Zeiss, LSM800).

Hematoxylin and eosin staining

Mouse skin was dissected and fixed with 4% paraformaldehyde overnight. The next day, the skin was immersed in 30% sucrose solution overnight, then embedded in Tissue-Tek O.C.T. compound (Sakura Finetek). The skin was sectioned on a cryostat at 10 μm. The sections were rinsed with PBS and then with distilled water, and stained with hematoxylin and eosin (Abcam, ab245880). The stained sections were covered with coverslips and then

imaged with a microscope (Axioplan 2, Carl Zeiss).

Cell culture and heterologous expression of ANO1

HEK293T cells and CHO cells were cultured in DMEM (10% FBS, 2 mM L-glutamine, Penicillin/streptomycin). To induce ANO1 expression in HEK293T or CHO cells, cells were transfected with mouse *Ano1*, *Mrgpra3*, *Mrgprc11* or *Mrgpra1* cDNA mixed with FuGene HD or XtremeGene HD transfection reagent (Roche Diagnostics, Penzberg, Germany). Transfected cells were plated onto glass coverslips. Their current responses were recorded 24 to 48 hr after transfection.

Primary cultures of DRG neurons

Primary cell cultures of DRG neurons were conducted as previously described [8]. Thoracic and lumbar DRGs were dissected from CTL, cKO mice and collected in cold culture medium (4ºC) containing a mixture of DMEM and F-12 solution, 10% fetal bovine serum (Gibco BRL), 1 mM sodium pyruvate, 50-100 ng/ml nerve growth factor (Alomon, Jerusalem, Israel), and 100 units/ml of penicillin/streptomycin. Ganglia were washed with culture medium and incubated for 30 min in a warm (37ºC) DMEM/F-12 mixture containing 1 mg/ml of collagenase (Type II; Worthington Biomedical). DRGs were then washed 3 times with Mg^{2+}- and Ca^{2+}-free Hank's solution and incubated with gentle shaking in Hank's solution containing 2.5 mg/ml of trypsin (Roche Diagnostics) for 30 min at 37ºC. The trypsin-containing solution was then centrifuged at 100 g for 10 min. The pellets obtained were washed gently 2-3 times with culture medium and suspended in culture medium. Then, cells gently triturated with a fire-polished Pasteur pipette were plated onto round glass coverslips (Fisher), which had been previously treated with poly-L-lysine (0.5 mg/ml), in small Petri dishes (35 x 12 mm). Cells were then placed in a 37ºC incubator in a 95% air/5% CO_2 atmosphere. Cells were used 2-4 days after plating.

Whole-cell patch clamp recordings

Whole-cell current recordings were obtained using a voltage clamp or a current clamp technique with an Axopatch 200B amplifier (Molecular Devices) as described previously [8]. Whole cells were formed after breaking the plasma membrane under the pipette tips. The resistance of glass pipettes was about 3 mΩ. Junctional potentials were canceled to zero. For recording currents in cell lines, the pipette solution contained (in mM): 140 NMDG-Cl, 2 $MgCl_2$, 2 ATP, and 0.3 GTP, adjusted to pH 7.2. The bath solution contained (in mM): 140 NMDG-Cl, 2 $MgCl_2$. For DRG neuron recordings, the pipette solution contained (in mM): 30 KCl, 110 K-Aspartate, 2 $MgCl_2$, 10 HEPES, adjusted to pH 7.2. The bath solution contained (in mM): 140 NaCl, 2 $MgCl_2$, 2 $CaCl_2$, 10 HEPES, adjusted to pH 7.2. The osmolarity of all solutions was adjusted to 290-300 mOsm by adding D-Mannitol. Holding potential was set at -60 mV. Whole-cell currents were amplified with Axopatch 200B (Molecular Device). The output of the amplifier was filterd at 1 kHz, digitized using Digidata 1440 (Molecular Devices), and stored in a personal computer.

Measurements of CQ-induced activity of DRG neurons in vivo

Experiments were conducted as previously described [7, 20, 24]. CaMKlla-dependent GCaMP6f mice were made by crossing CaMKlla-CRE (Jackson lab, #005359) mice and GCaMP6f (Jackson lab, #024105) mice, and $CaMKlla^{CRE}GCaMP6f^{+/-}$ were used for the experiment. For two-photon imaging experiments, male mice older than 3 months were intraperitoneally injected and anesthetized with a mixture of Zoletil 50 and Rompun (Bayer) at a ratio of 2:1. The body temperatures of mice were maintained at about 37°C with a heating pad. After deep anesthesia, the back of mice was shaved, and the skin was incised upto about 2 cm based on the pelvic bones. The vertebrae of L3 to L6 were exposed. The vertebrae between the ribs and the pelvic bones were clamped. The mice were gently tilted so that the DRGs could be as horizontal as possible. A well to hold artificial cerebrospinal fluid (ACSF) was made with resin around the custom-made clamp and the skin. With a small

rongeur, transverse process and spinous process covering the L4 DRG were carefully removed. Bleeding was controlled with continuous irrigation using normal saline and ACSF. The well was filled with ACSF and the L4 DRG of the mice was placed under a two photon microscope. The ACSF contained (in mM): 135 NaCl, 5.4 KCl, 1 $MgCl_2$, 1.8 $CaCl_2$, 5 HEPES, and the pH was adjusted between 7.3-7.5 using 1N KOH.

For chemical stimulus, 10 µl of CQ (40 mg/ml) with 2 mM MONNA or vehicle (0.2% DMSO) were injected into the plantar of the ipsilateral hind paw, and two-photon imaging was started right after the chemical injection. To asses the total number of functional neurons in DRGs, 250 mM of KCl dissolved in ACSF were treated over DRG in the well.

Two-photon imaging was performed on a Leica TCS SP5 microscope combined with a Maitai (Spectra Physics) mode-locked Ti-sapphire laser (920nm for GFP). Emission of green light (500-550nm) was collected. Fluorescence images were acquired through a 20x water-immersion objective (Leica HCX APO L 20 x 1.0; 1.0 NA); 512 x 512 pixel images were acquired at 0.76 Hz. Total 550 image frames were collected for each experiments, right after intraplantar chemical injection. All images were acquired at a single focal plane near surface of DRG.

Total 6 mice were used in the analysis, 3 mice for CQ injection and other 3 mice for CQ coinjected with MONNA. All images were analyzed using the ImageJ (NIH). Regions of interest were chosen and calcium signals were measured and expressed as F/F_0 as a function of frames of each images. Fluorescence signals with distinct Ca^{2+} spikes or with sudden increase followed by gradual decrease were counted as responders. The background fluorescence signals with $F/F_0 < 1.0$ or with a slow and gradual increase were considered as non-responders and excluded.

YFP fluorescence assay

HEK293T cells or CHO-K1 cells were plated on a poly-L-lysine coated 8-well plate. The

next day, cells were transfected with *Yfp-H148Q/I152L/F46L* and/or *Ano1* and/or one of *MrgprA3, MrgprC11,* and *MrgprA1*. After 48 hours of transfection, the medium was washed with the pre-warmed Na-HEPES solution. Then YFP fluorescence was measured with a confocal microscope (LSM800, Carl Zeiss). CQ (1 mM), SLIGRL (100 μM), or bilirubin (100 μM) –containing NaI-HEPES solution was applied to the cells. The YFP fluorescence was imaged with excitation 508 nm and emission 524 nm. After the experiments, the fluorescence intensities of the cells were analyzed using the Image J program (NIH). Regions of interest were chosen. The fluorescence extinction was measured in the regions and expressed as F/F_0 as a function of frames of each image. Na-HEPES solution contained (in mM) 140 NaCl, 10 HEPES, 2 $MgCl_2$, 2 $CaCl_2$, and 10 D-Mannitol (pH 7.2). Na-I-HEPES solution contained (in mM) 140 NaI, 10 HEPES, 2 $MgCl_2$, 2 $CaCl_2$, and 10 D-Mannitol (pH 7.2). We added the NaI solution with twice the volume of the Na-HEPES solution. Therefore, the concentration ratio of Cl^- and I^- in the bath was 1:2, with the final concentrations of Cl^- and I^- in the bath solution were 46.7 and 93.3 mM, respectively.

Statistics

Data in the figures are shown as the mean ± SEM. To compare multiple means, one-way ANOVA was used with Tukey's or Bonferroni's post hoc test. An unpaired or paired two-tailed Student's *t*-test was used to compare two means. The Chi-square test was used to compare the effects of two variables. P values of less than 0.05 were considered significantly different.

AUTHOR CONTRIBUTIONS

HK performed scratching behavior tests, *in-vivo* Ca^{2+} imaging, and rescue experiments, HK carried out skin immunohistochemistry. HC and HK performed electrophysiological

experiments, BL and HL performed behavioral tests, KK carried out histology, WS performed behavior tests, YS supervised animal experiments, SJ and JNW carried out *in-vivo* Ca^{2+} imaging, XD carried out immunofluorescence experiments, and UO initiated, designed the study, and wrote the manuscript.

ACKNOWLEDGEMENTS

This study was supported by the National Research Foundation of Korea (2020R1A3A300192911).

Conflict of interest statement: The authors have declared that no conflict of interest exists.

REFERENCES

[1] Akiyama T, Carstens MI, Carstens E. Enhanced scratching evoked by PAR-2 agonist and 5-HT but not histamine in a mouse model of chronic dry skin itch. Pain 2010;151(2):378-383.

[2] Bautista DM, Wilson SR, Hoon MA. Why we scratch an itch: the molecules, cells and circuits of itch. Nat Neurosci 2014;17(2):175-182.

[3] Bishop GH. The skin as an organ of senses with special reference to the itching sensation. J Invest Dermatol 1948;11(2):143-154.

[4] Britschgi A, Bill A, Brinkhaus H, Rothwell C, Clay I, Duss S, Rebhan M, Raman P, Guy CT, Wetzel K, George E, Popa MO, Lilley S, Choudhury H, Gosling M, Wang L, Fitzgerald S, Borawski J, Baffoe J, Labow M, Gaither LA, Bentires-Alj M. Calcium-activated chloride channel ANO1 promotes breast cancer progression by activating EGFR and CAMK signaling. Proc Natl Acad Sci U S A 2013;110(11):E1026-1034.

[5] Caputo A, Caci E, Ferrera L, Pedemonte N, Barsanti C, Sondo E, Pfeffer U, Ravazzolo R, Zegarra-Moran O, Galietta LJ. TMEM16A, a membrane protein associated with calcium-dependent chloride channel activity. Science 2008;322(5901):590-594.

[6] Cha JY, Wee J, Jung J, Jang Y, Lee B, Hong GS, Chang BC, Choi YL, Shin YK, Min HY, Lee HY, Na TY, Lee MO, Oh U. Anoctamin 1 (TMEM16A) is essential for testosterone-induced prostate hyperplasia. PNAS 2015;112(31):9722-9727.

[7] Chisholm KI, Khovanov N, Lopes DM, La Russa F, McMahon SB. Large Scale In Vivo Recording of Sensory Neuron Activity with GCaMP6. eNeuro 2018;5(1).

[8] Cho H, Yang YD, Lee J, Lee B, Kim T, Jang Y, Back SK, Na HS, Harfe BD, Wang F, Raouf R, Wood JN, Oh U. The calcium-activated chloride channel anoctamin 1 acts as a heat sensor in nociceptive neurons. Nat Neurosci 2012;15(7):1015-1021.

[9] Dong X, Dong X. Peripheral and Central Mechanisms of Itch. Neuron 2018;98(3):482-494.

[10] Gombash Lampe SE, Kaspar BK, Foust KD. Intravenous injections in neonatal mice. J Vis Exp 2014(93):e52037.

[11] Han L, Ma C, Liu Q, Weng HJ, Cui Y, Tang Z, Kim Y, Nie H, Qu L, Patel KN, Li Z, McNeil B, He S, Guan Y, Xiao B, Lamotte RH, Dong X. A subpopulation of nociceptors specifically linked to itch. Nat Neurosci 2013;16(2):174-182.

[12] Hashimoto T, Yosipovitch G. Itching as a systemic disease. J Allergy Clin Immunol 2019;144(2):375-380.

[13] Hong GS, Lee SH, Lee B, Choi JH, Oh SJ, Jang Y, Hwang EM, Kim H, Jung J, Kim IB, Oh U. ANO1/TMEM16A regulates process maturation in radial glial cells in the developing brain. Proc Natl Acad Sci U S A 2019;116(25):12494-12499.

[14] Ikoma A, Steinhoff M, Stander S, Yosipovitch G, Schmelz M. The neurobiology of itch. Nat Rev Neurosci 2006;7(7):535-547.

[15] Imamachi N, Park GH, Lee H, Anderson DJ, Simon MI, Basbaum AI, Han SK. TRPV1-expressing primary afferents generate behavioral responses to pruritogens via multiple mechanisms. Proc Natl Acad Sci U S A 2009;106(27):11330-11335.

[16] Jang Y, Oh U. Anoctamin 1 in secretory epithelia. Cell Calcium 2014;55(6):355-361.

[17] Jin X, Shah S, Liu Y, Zhang H, Lees M, Fu Z, Lippiat JD, Beech DJ, Sivaprasadarao A, Baldwin SA, Zhang H, Gamper N. Activation of the Cl- channel ANO1 by localized calcium signals in nociceptive sensory neurons requires coupling with the IP3 receptor. Science signaling 2013;6(290):ra73.

[18] Kawabata A, Saifeddine M, Al-Ani B, Leblond L, Hollenberg MD. Evaluation of proteinase-activated receptor-1 (PAR1) agonists and antagonists using a cultured cell receptor desensitization assay: activation of PAR2 by PAR1-targeted ligands. J Pharmacol Exp Ther 1999;288(1):358-370.

[19] Kim SJ, Park GH, Kim D, Lee J, Min H, Wall E, Lee CJ, Simon MI, Lee SJ, Han SK. Analysis of cellular and behavioral responses to imiquimod reveals a unique itch pathway in transient receptor potential vanilloid 1 (TRPV1)-expressing neurons. Proc Natl Acad Sci U S A 2011;108(8):3371-3376.

[20] Kim YS, Anderson M, Park K, Zheng Q, Agarwal A, Gong C, Saijilafu, Young L, He S, LaVinka PC, Zhou F, Bergles D, Hanani M, Guan Y, Spray DC, Dong X. Coupled Activation of Primary Sensory Neurons Contributes to Chronic Pain. Neuron 2016;91(5):1085-1096.

[21] Klein PA, Clark RA. An evidence-based review of the efficacy of antihistamines in relieving pruritus in atopic dermatitis. Arch Dermatol 1999;135(12):1522-1525.

[22] LaMotte RH, Dong X, Ringkamp M. Sensory neurons and circuits mediating itch. Nat Rev Neurosci 2014;15(1):19-31.

[23] Lee B, Cho H, Jung J, Yang YD, Yang DJ, Oh U. Anoctamin 1 contributes to inflammatory and nerve-injury induced hypersensitivity. Mol Pain 2014;10(1):5.

[24] Lee JH, Shin HS, Lee KH, Chung S. LFP-guided targeting of a cortical barrel column for in vivo two-photon calcium imaging. Sci Rep 2015;5:15905.

[25] Liu B, Linley JE, Du X, Zhang X, Ooi L, Zhang H, Gamper N. The acute nociceptive signals induced by bradykinin in rat sensory neurons are mediated by inhibition of M-type K+ channels and activation of Ca2+-activated Cl- channels. J Clin Invest 2010;120(4):1240-1252.

[26] Liu Q, Tang Z, Surdenikova L, Kim S, Patel KN, Kim A, Ru F, Guan Y, Weng HJ, Geng Y, Undem BJ, Kollarik M, Chen ZF, Anderson DJ, Dong X. Sensory neuron-specific GPCR Mrgprs are itch receptors mediating chloroquine-induced pruritus. Cell 2009;139(7):1353-1365.

[27] Liu Q, Weng HJ, Patel KN, Tang Z, Bai H, Steinhoff M, Dong X. The distinct roles of two GPCRs, MrgprC11 and PAR2, in itch and hyperalgesia. Science signaling 2011;4(181):ra45.

[28] Liu T, Ji RR. New insights into the mechanisms of itch: are pain and itch controlled by distinct mechanisms? Pflugers Arch 2013;465(12):1671-1685.

[29] Liu T, Xu ZZ, Park CK, Berta T, Ji RR. Toll-like receptor 7 mediates pruritus. Nat Neurosci 2010;13(12):1460-1462.

[30] Liu W, Lu M, Liu B, Huang Y, Wang K. Inhibition of Ca(2+)-activated Cl(-) channel ANO1/TMEM16A expression suppresses tumor growth and invasiveness in human

prostate carcinoma. Cancer Lett 2012;326(1):41-51.

[31] Lukacs V, Yudin Y, Hammond GR, Sharma E, Fukami K, Rohacs T. Distinctive changes in plasma membrane phosphoinositides underlie differential regulation of TRPV1 in nociceptive neurons. The Journal of neuroscience : the official journal of the Society for Neuroscience 2013;33(28):11451-11463.

[32] Meixiong J, Vasavda C, Green D, Zheng Q, Qi L, Kwatra SG, Hamilton JP, Snyder SH, Dong X. Identification of a bilirubin receptor that may mediate a component of cholestatic itch. Elife 2019;8.

[33] Meixiong J, Vasavda C, Snyder SH, Dong X. MRGPRX4 is a G protein-coupled receptor activated by bile acids that may contribute to cholestatic pruritus. Proc Natl Acad Sci U S A 2019;116(21):10525-10530.

[34] Mishra RK, Li Y, Ricardo AC, Yang W, Keane M, Cuevas M, Christenson R, deFilippi C, Chen J, He J, Kallem RR, Raj DS, Schelling JR, Wright J, Go AS, Shlipak MG, Chronic Renal Insufficiency Cohort I. Association of N-terminal pro-B-type natriuretic peptide with left ventricular structure and function in chronic kidney disease (from the Chronic Renal Insufficiency Cohort [CRIC]). Am J Cardiol 2013;111(3):432-438.

[35] Miyamoto T, Nojima H, Shinkado T, Nakahashi T, Kuraishi Y. Itch-associated response induced by experimental dry skin in mice. Jpn J Pharmacol 2002;88(3):285-292.

[36] Morita T, McClain SP, Batia LM, Pellegrino M, Wilson SR, Kienzler MA, Lyman K, Olsen AS, Wong JF, Stucky CL, Brem RB, Bautista DM. HTR7 Mediates Serotonergic Acute and Chronic Itch. Neuron 2015;87(1):124-138.

[37] Namkung W, Phuan PW, Verkman AS. TMEM16A inhibitors reveal TMEM16A as a minor component of calcium-activated chloride channel conductance in airway and intestinal epithelial cells. The Journal of biological chemistry 2011;286(3):2365-2374.

[38] Oh SJ, Hwang SJ, Jung J, Yu K, Kim J, Choi JY, Hartzell HC, Roh EJ, Lee CJ. MONNA, a potent and selective blocker for transmembrane protein with unknown function 16/anoctamin-1. Mol Pharmacol 2013;84(5):726-735.

[39] Ormö M, Cubitt AB, Kallio K, Gross LA, Tsien RY, Remington SJ. Crystal structure of the Aequorea victoria green fluorescent protein. Science 1996;273(5280):1392-1395.

[40] Pedemonte N, Galietta LJ. Structure and function of TMEM16 proteins (anoctamins). Physiol Rev 2014;94(2):419-459.

[41] Roberson DP, Gudes S, Sprague JM, Patoski HA, Robson VK, Blasl F, Duan B, Oh SB, Bean BP, Ma Q, Binshtok AM, Woolf CJ. Activity-dependent silencing reveals functionally distinct itch-generating sensory neurons. Nat Neurosci 2013;16(7):910-918.

[42] Ru F, Sun H, Jurcakova D, Herbstsomer RA, Meixong J, Dong X, Undem BJ. Mechanisms of pruritogen-induced activation of itch nerves in isolated mouse skin. J Physiol 2017;595(11):3651-3666.

[43] Sakai K, Sanders KM, Youssef MR, Yanushefski KM, Jensen L, Yosipovitch G, Akiyama T. Mouse model of imiquimod-induced psoriatic itch. Pain 2016;157(11):2536-2543.

[44] Schmelz M, Schmelz M. Itch and pain

How pain becomes itch. Neurosci Biobehav Rev 2010;34(2):171-176.

[45] Schmelz M, Schmidt R, Bickel A, Handwerker HO, Torebjork HE. Specific C-receptors for itch in human skin. The Journal of neuroscience : the official journal of the Society for Neuroscience 1997;17(20):8003-8008.

[46] Schroeder BC, Cheng T, Jan YN, Jan LY. Expression cloning of TMEM16A as a calcium-activated chloride channel subunit. Cell 2008;134(6):1019-1029.

[47] Shah S, Carver CM, Mullen P, Milne S, Lukacs V, Shapiro MS, Gamper N. Local Ca(2+)

signals couple activation of TRPV1 and ANO1 sensory ion channels. Science signaling 2020;13(629).

[48] Sharif B, Ase AR, Ribeiro-da-Silva A, Séguéla P. Differential Coding of Itch and Pain by a Subpopulation of Primary Afferent Neurons. Neuron 2020;106(6):940-951.e944.

[49] Shim WS, Oh U. Histamine-induced itch and its relationship with pain. Mol Pain 2008;4:29.

[50] Shim WS, Tak MH, Lee MH, Kim M, Kim M, Koo JY, Lee CH, Kim M, Oh U. TRPV1 mediates histamine-induced itching via the activation of phospholipase A2 and 12-lipoxygenase. The Journal of neuroscience : the official journal of the Society for Neuroscience 2007;27(9):2331-2337.

[51] Sikand P, Dong X, LaMotte RH. BAM8-22 peptide produces itch and nociceptive sensations in humans independent of histamine release. The Journal of neuroscience : the official journal of the Society for Neuroscience 2011;31(20):7563-7567.

[52] Steinhoff M, Neisius U, Ikoma A, Fartasch M, Heyer G, Skov PS, Luger TA, Schmelz M. Proteinase-activated receptor-2 mediates itch: a novel pathway for pruritus in human skin. The Journal of neuroscience : the official journal of the Society for Neuroscience 2003;23(15):6176-6180.

[53] Sun S, Xu Q, Guo C, Guan Y, Liu Q, Dong X. Leaky Gate Model: Intensity-Dependent Coding of Pain and Itch in the Spinal Cord. Neuron 2017;93(4):840-853 e845.

[54] Sun YG, Chen ZF. A gastrin-releasing peptide receptor mediates the itch sensation in the spinal cord. Nature 2007;448(7154):700-703.

[55] Takayama Y, Uta D, Furue H, Tominaga M. Pain-enhancing mechanism through interaction between TRPV1 and anoctamin 1 in sensory neurons. Proc Natl Acad Sci U S A 2015;112(16):5213-5218.

[56] Verkman AS, Galietta LJ. Chloride channels as drug targets. Nat Rev Drug Discov

2009;8(2):153-171.

[57] Wilson SR, Gerhold KA, Bifolck-Fisher A, Liu Q, Patel KN, Dong X, Bautista DM. TRPA1 is required for histamine-independent, Mas-related G protein-coupled receptor-mediated itch. Nat Neurosci 2011;14(5):595-602.

[58] Wilson SR, Nelson AM, Batia L, Morita T, Estandian D, Owens DM, Lumpkin EA, Bautista DM. The ion channel TRPA1 is required for chronic itch. The Journal of neuroscience : the official journal of the Society for Neuroscience 2013;33(22):9283-9294.

[59] Yamaguchi T, Nagasawa T, Satoh M, Kuraishi Y. Itch-associated response induced by intradermal serotonin through 5-HT2 receptors in mice. Neurosci Res 1999;35(2):77-83.

[60] Yang YD, Cho H, Koo JY, Tak MH, Cho Y, Shim WS, Park SP, Lee J, Lee B, Kim BM, Raouf R, Shin YK, Oh U. TMEM16A confers receptor-activated calcium-dependent chloride conductance. Nature 2008;455(7217):1210-1215.

[61] Yosipovitch G, Bernhard JD. Clinical practice. Chronic pruritus. N Engl J Med 2013;368(17):1625-1634.

[62] Yosipovitch G, Goon A, Wee J, Chan YH, Goh CL. The prevalence and clinical characteristics of pruritus among patients with extensive psoriasis. Br J Dermatol 2000;143(5):969-973.

[63] Zhu Y, Hanson CE, Liu Q, Han L. Mrgprs activation is required for chronic itch conditions in mice. Itch (Phila) 2017;2(3):e9.

FIGURE LEGENDS

Figure 1. Genetic deletion of *Ano1* in DRGs reduces scratching behaviors in Mrgprs dependent itch models.

(**A**) Chloroquine (CQ) and SLIGRL induced scratching in littermate control (CTL) and $Adv^{CRE}Ano1^{fl/fl}$ (cKO) mice. Scratching behaviors were counted for 30 min in CTL and cKO mice after subcutaneous injection of vehicle (100 μl), SLIGRL (65 μg/100 μl), or CQ (200 μg/100 μl) into the nape of the neck. * $p < 0.05$, ** $p < 0.01$, *** $p < 0.001$, one-way ANOVA followed by Tukey's post hoc test. Data represent the mean ± SEM.

(**B**) CQ (200 μg/100 μl) and CQ + MONNA (35 μg/100 μl) induced scratching in CTL mice after subcutaneous injection into the nape of the neck. ** $p < 0.01$, Student's *t*-test.

(**C**) Histamine (His), endothelin-1 (ET-1), and 5-HT induced scratching in CTL and cKO mice after subcutaneous injection of vehicle (100 μl), histamine (200 μg/100μl), endothelin-1 (125 ng/100μl), and 5-HT (20 μg/100μl) into the nape of the neck. Data for Veh injection in each group are identical. ns: not significant, * $p < 0.05$, ** $p < 0.01$, *** $p < 0.001$, one-way ANOVA followed by Tukey's post hoc test.

(**D**) Bilirubin-induced scratching in CTL and cKO mice after the subcutaneous injection of vehicle (50 μl) and bilirubin (60 μg/50 μl) into the nape of the neck. ns : not significant, * $p < 0.05$, *** $p < 0.001$, one-way ANOVA followed by Tukey's post hoc test.

(**E**) Dry skin-evoked scratching in CTL and cKO mice in 3 and 5 days after the repeated treatments of acetone, ether, and water (AEW) on the cheek. Total time spent scratching was recorded for 30 min. The vehicle group was treated with water only. * $p < 0.05$, ** $p < 0.01$, *** $p < 0.001$, ns : not significant, one-way ANOVA followed by Tukey's post hoc test.

Figure 2. Genetic ablation of *Ano1* reduces the AEW-induced epidermal hyperplasia.

(**A-B**) H&E staining of the cheek skin of CTL (A) and cKO mice (B) after 5-day AEW treatment. Water was applied for control on the contralateral cheek of mice. Arrows indicate the epidermis. Scale bar: 50 μm.

(**C**) Comparison of the thickness of the epidermis after AEW in both CTL and cKO mice. ns: not significant, *** $p < 0.001$, one-way ANOVA followed by Bonferroni's post hoc test.

Figure 3. The expression patterns of ANO1, MrgprA3, and H1R in DRG neurons.

(A) L4-L6 DRG sections from *MrgprA3*$^{GFP\text{-}Cre}$ transgenic mice were double-stained with antibodies to mouse ANO1 (red) and GFP (green). Scale bar: 20 μm.

(B) Venn diagrams showing the proportion of ANO1 and MrgprA3 positive neurons.

(C) L4-L6 DRG sections double-stained with antibodies to mouse ANO1 (red) and H1R (green). Scale bar: 100 μm.

(D) Venn diagrams showing the proportion of ANO1 and H1R positive neurons.

Figure 4. ANO1 mediates the CQ and SLIGRL-induced excitation of DRG neurons.

(**A**) Representative traces showing the depolarization with action potential firings evoked by CQ (1 mM) application in a DRG neuron isolated from CTL mice but not in a DRG neuron from cKO mice. *Right*, pie charts of DRG neurons of CTL and *Ano1* cKO mice illustrate the number of cells responsive to the CQ application. $p < 0.05$, Chi-square test.

(**B**) The excitation of DRG neurons induced by CQ (1 mM) and its block by the treatment with ANO1 specific blocker, MONNA (10 μM). *Right*, a summary of the inhibition of

CQ-induced action potential by MONNA. * $p < 0.05$, Student's *t*-test.

(**C**) SLIGRL (1 mM) evoked the depolarization with action potential firings in a DRG neuron isolated from CTL mice but not in a DRG neuron from cKO mice. *Right*, pie charts of DRG neurons of CTL and cKO mice illustrate the number of cells responsive to SLIGRL. $p < 0.05$, Chi-square test.

(**D**) SLIGRL-induced action potential firings in DRG neurons of CTL mice was significantly attenuated by 10 □M MONNA. * $p < 0.05$, Student's *t*-test.

Figure 5. The pharmacological block of ANO1 inhibits CQ-induced Ca^{2+} signals of DRG neurons *in vivo*.

(**A**) Representative fluorescence images of DRG neurons (arrowheads) that showed GCaMP-dependent Ca^{2+} signals before (left) and after (right) the CQ injection. Fluorescence intensities of GCaMP6f-expressing DRG neurons were measured with a two-photon microscope after CQ injection (400 μg/10 μl) into the ipsilateral hind paw. Scale bars: 20 μm.

(**B**) Representative fluorescence images of GCaMP6f-expressing DRG neurons after direct KCl (250 mM) application to a DRG. Scale bar: 100 μm.

(**C-D**) GCaMP optical *in-vivo* Ca^{2+} imaging of DRG neurons in L4 DRGs in *CaMKIIa*^{CRE}*GCaMP6f*$^{fl/+}$ mice. CQ (400 μg/10 μl) injection into the ipsilateral plantar of the hindlimb (injected at 0 min, arrow) evoked Ca^{2+} responses in DRG neurons (C), which was markedly reduced when CQ + MONNA (2 mM) were injected (D). Only responders were presented (see Methods).

(**E**) The average values of responders from both groups were plotted against the fluorescence intensity (F/F_0) for every 30 seconds (CQ, n=60; CQ+MONNA, n=56). * $p < 0.05$, ** p

< 0.01, Student's *t*-test.

(**F**) Pie charts of DRG neurons of *CaMKIIa*^{CRE}*GCaMP6f*$^{fl+}$ mice responding to the intraplantar injecton of CQ or CQ+MONNA. After the CQ injection, 250 mM KCl was applied to assess the total numbers of DRG neurons. $p < 0.05$, Chi-square test.

Figure 6. Agonist stimulations of Mrgprs activate ANO1 in the heterologous expression system.

(A) Representative traces of 500 μM CQ-induced currents in HEK293T cells transfected with *Mrgpra3* and *Ano1*, *Mrgpra3* alone, or *Ano1* alone.

(**B**) A summary of ANO1 currents induced by CQ in *Mrgpra3* and *Ano1* expressing cells. * $p < 0.05$, one-way ANOVA followed by Tukey's post hoc test.

(**C**) Representative traces of 500 μM SLIGRL-induced currents in CHO cells transfected with *Mrgprc11* and *Ano1*, *Mrgprc11* alone, or *Ano1* alone.

(**D**) A summary of MrgprC11-stimulated ANO1 currents by SLIGRL. * $p < 0.05$, one-way ANOVA followed by Tukey's post hoc test.

(**E**) Representative traces of 50 μM bilirubin-induced currents in HEK293T cells transfected with *Mrgpra1* and *Ano1*, *Mrgpra1* alone, or *Ano1* alone.

(**F**) A summary of MrgprA1 stimulated ANO1 currents by bilirubin. * $p < 0.05$, one-way ANOVA followed by Tukey's post hoc test.

Figure 7. Stimulation of Mrgprs quenches the YFP fluorescence in cells expressing *Ano1* and *Mrgprs*.

(**A**) YFP fluorescence traces in YFP-H148Q/I152L/F46L-HEK293T cells expressing

MrgprA3 and *Ano1*, *Ano1* alone, or *MrgprA3* alone after 1 mM CQ treatment. (right) A summary of quenching ratios of the HEK293T cells expressing *MrgprA3* and *Ano1*, *Ano1* alone, or *MrgprA3* alone after 1 mM CQ treatment. *** $p < 0.001$, one-way ANOVA followed by Tukey's post hoc test.

(**B**) YFP fluorescence traces of YFP-H148Q/I152L/F46L-CHO-K1 cells expressing *MrgprC11* and *Ano1*, *Ano1* alone, or *MrgprC11* alone after 100 μM SLIGRL treatment. (right) A summary of quenching ratios of the CHO-K1 cells expressing *MrgprC11* and *Ano1*, *Ano1* alone, or *MrgprC11* alone after 100 μM SLIGRL treatment. *** $p < 0.001$, one-way ANOVA followed by Tukey's post hoc test.

(**C**) YFP fluorescence traces in YFP-H148Q/I152L/F46L-HEK293T cells expressing *MrgprA1* and *Ano1*, *Ano1* alone, or *MrgprA1* alone after 100 μM bilirubin treatment. (right) A summary of quenching ratios of the HEK293T cells expressing *MrgprC11* and *Ano1*, *Ano1* alone, or *MrgprC11* alone after 100 μM bilirubin treatment. *** $p < 0.001$, one-way ANOVA followed by Tukey's post hoc test.

Figure 8. Overexpression of *Ano1* in the *Ano1* cKO mice rescues the impaired scratching behavior of cKO mice.

(**A**) Immunofluorescence images of L4-L6 DRG neurons from CTL and *Ano1* cKO mice injected with AAV2-hSyn-mCherry or AAV2-hSyn-Ano1-mCherry virus. Scale bars: 20 μm.

(**B**) A summary of scratching responses to CQ (400 μg/100 μl) of AAV2-hSyn-mCherry or AAV2-hSyn-ANO1-mCherry-treated CTL and *Ano1* cKO mice. Note that the CQ-induced scratching was reduced in *Ano1* cKO mice treated with AAV2-hSyn-mCherry virus, which was rescued in *Ano1* cKO mice when treated with AAV2-hSyn-Ano1-

mCherry virus. * $p < 0.05$, ns : not significant, Student's *t*-test.

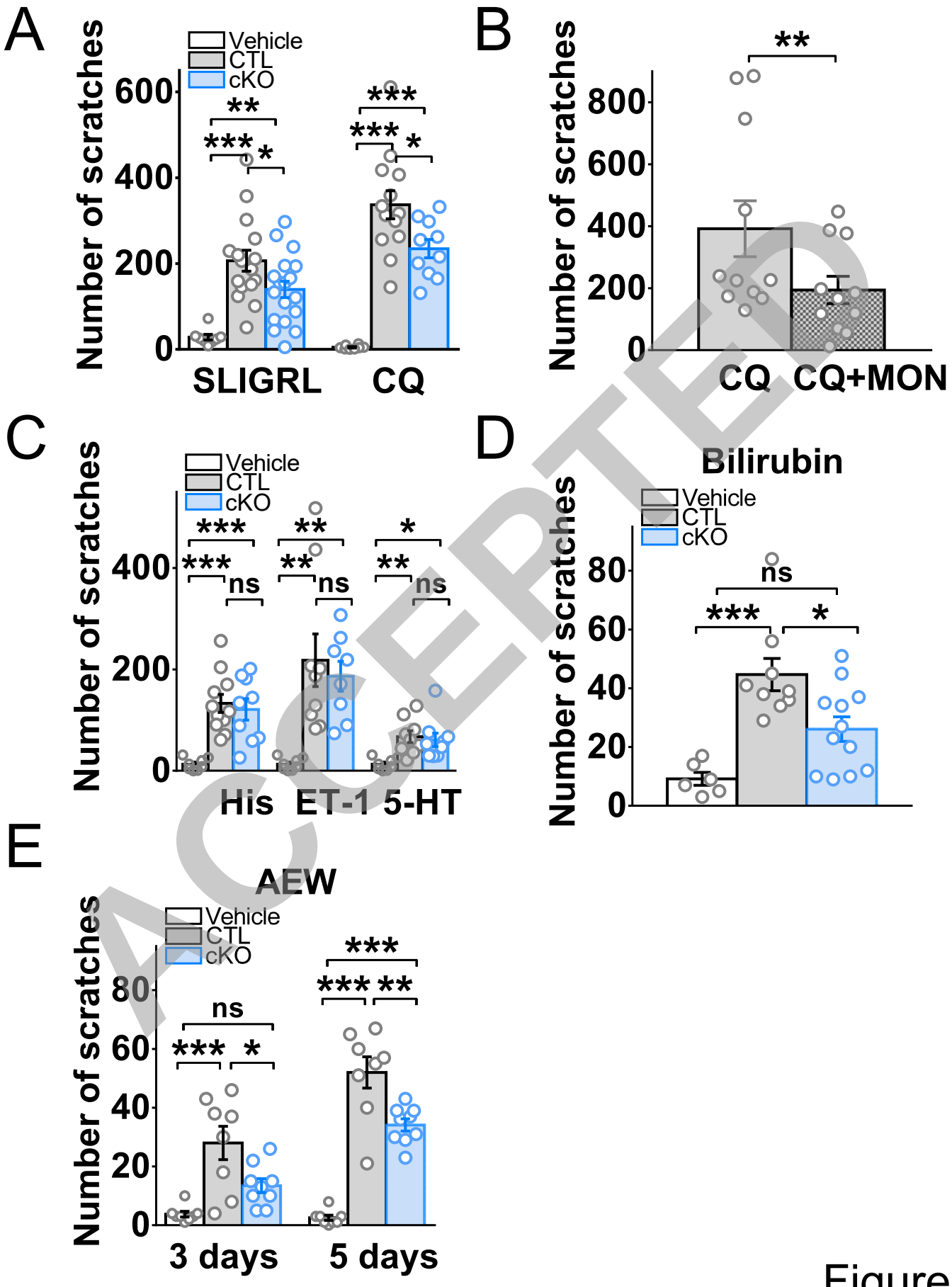

Figure 1

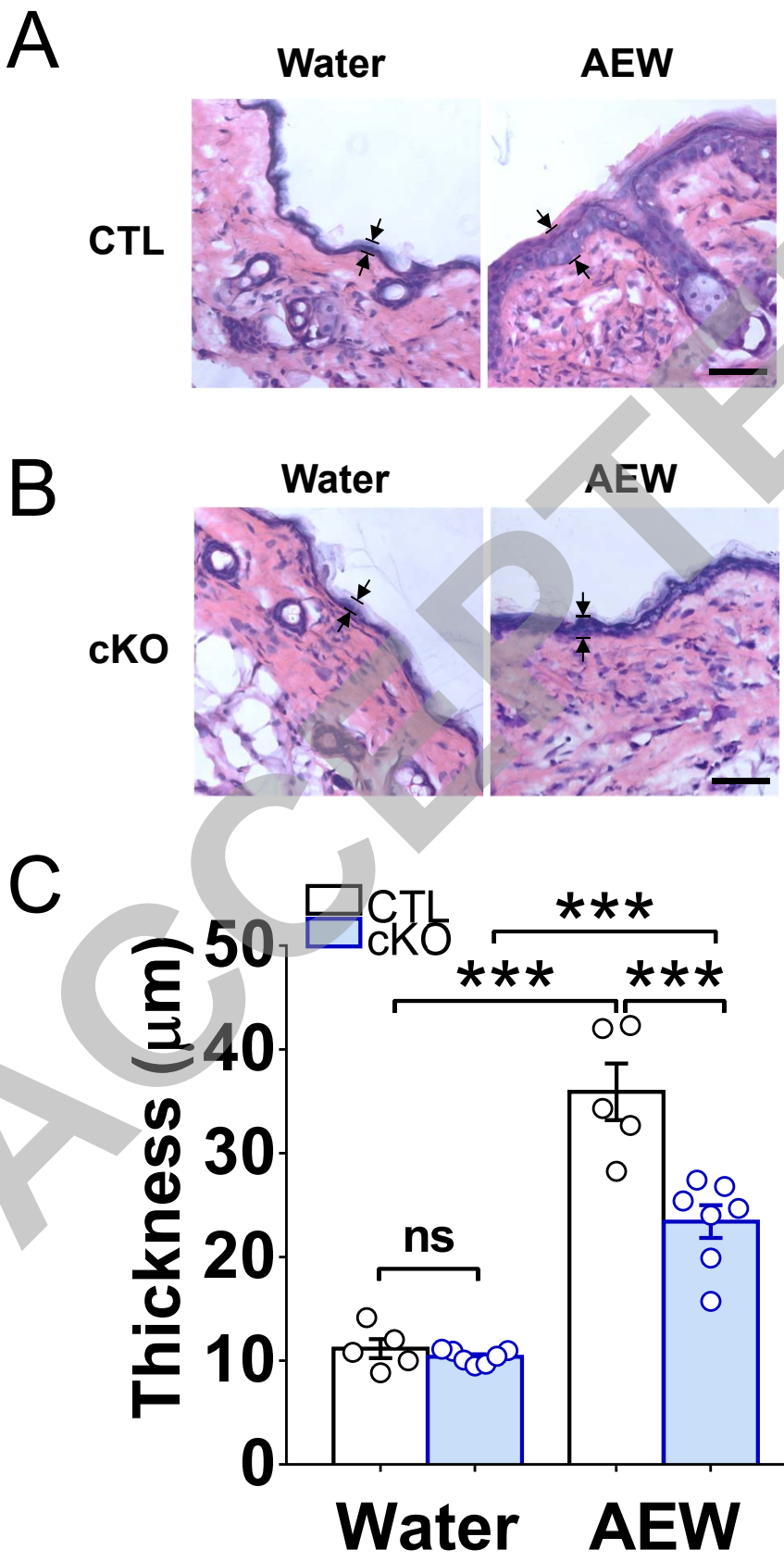

Figure 2

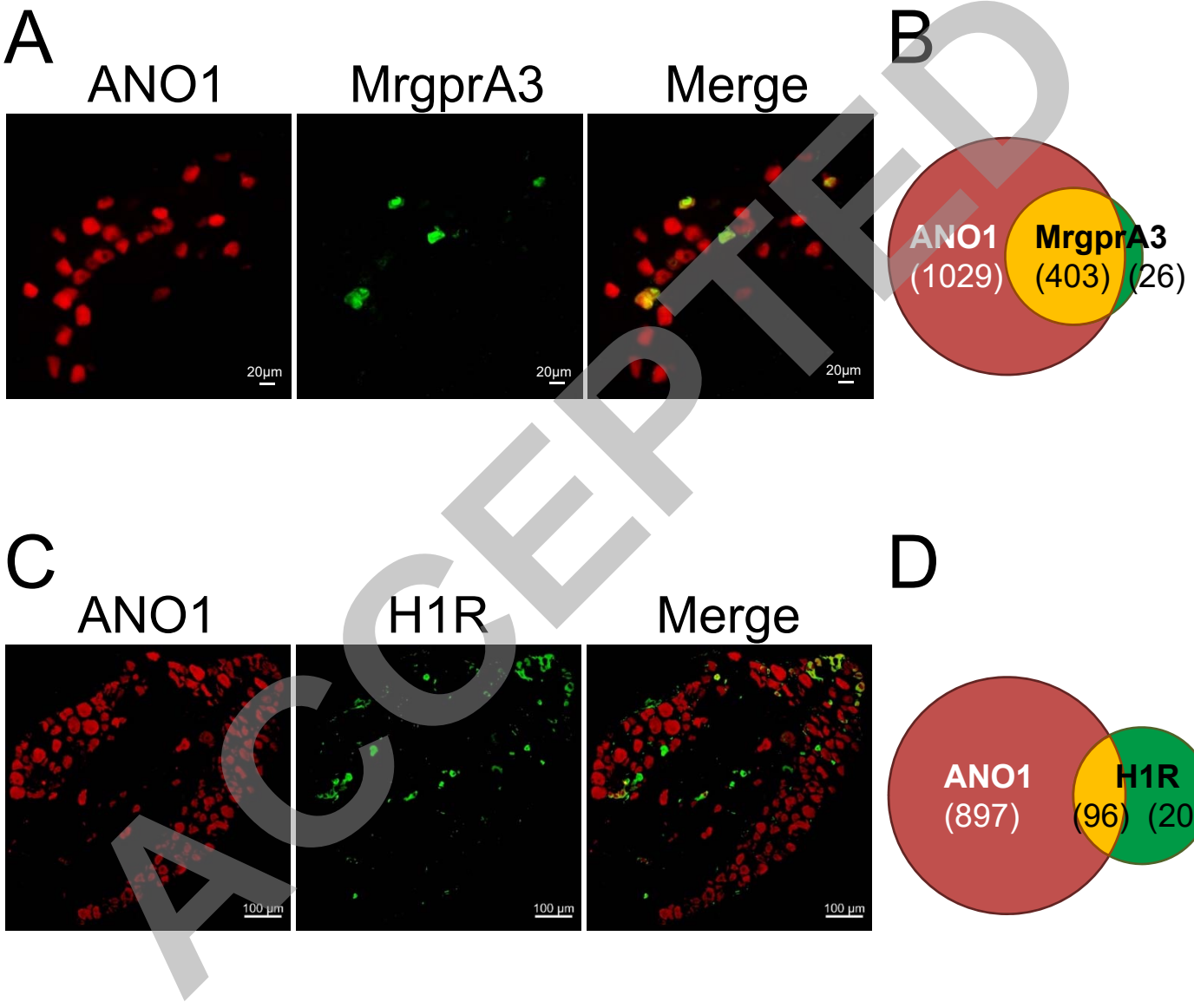

Figure 3

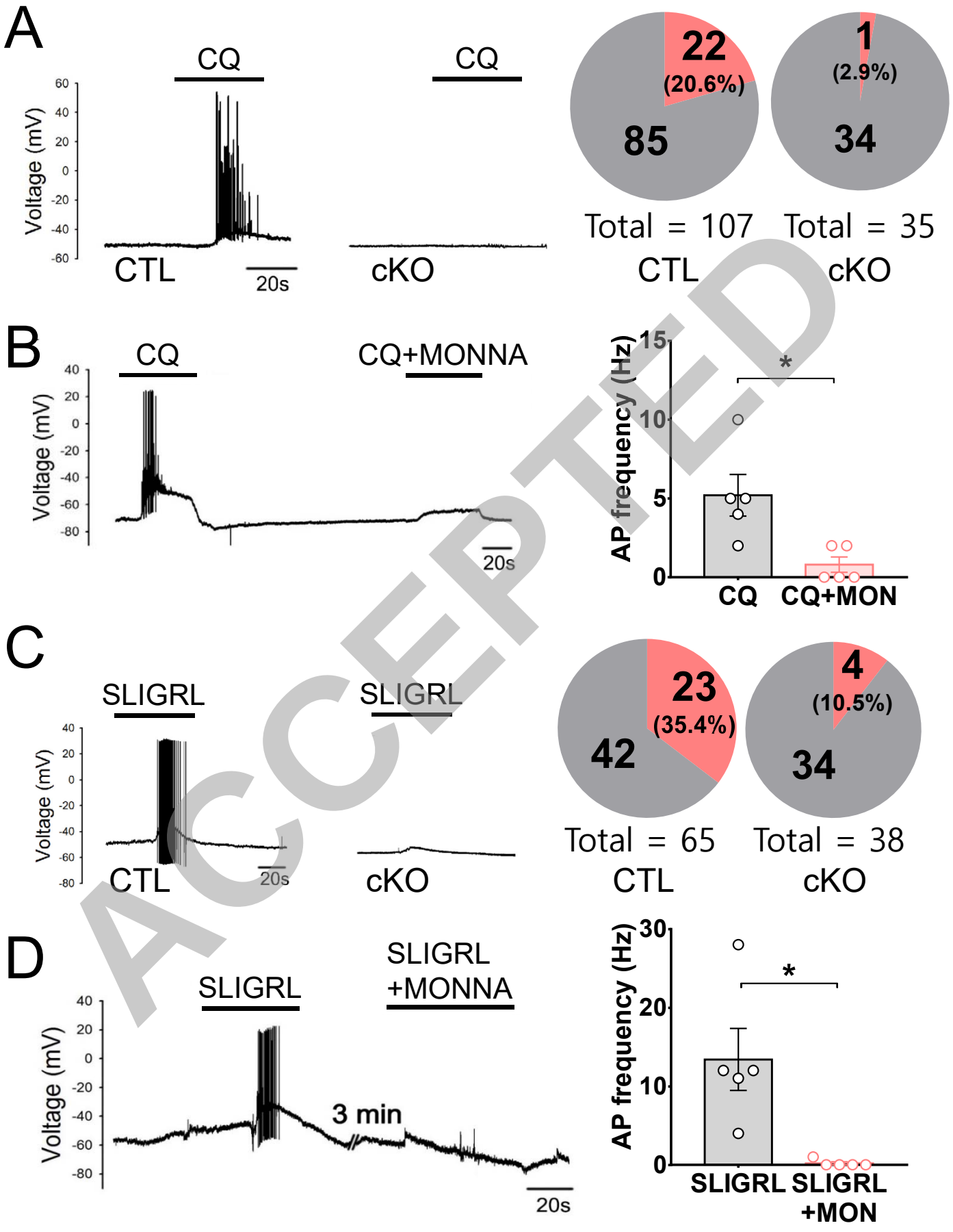

Figure 4

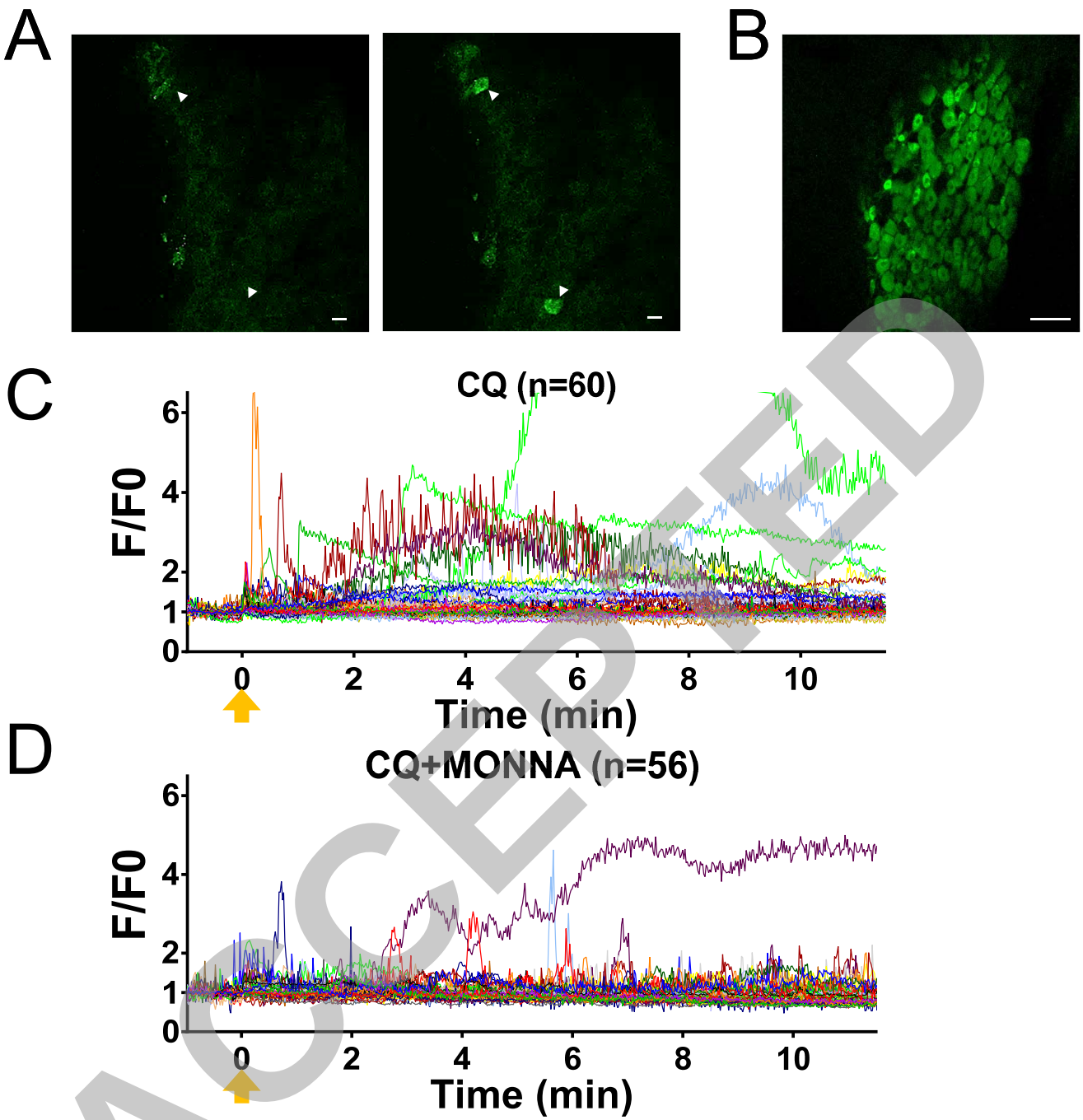

Figure 5

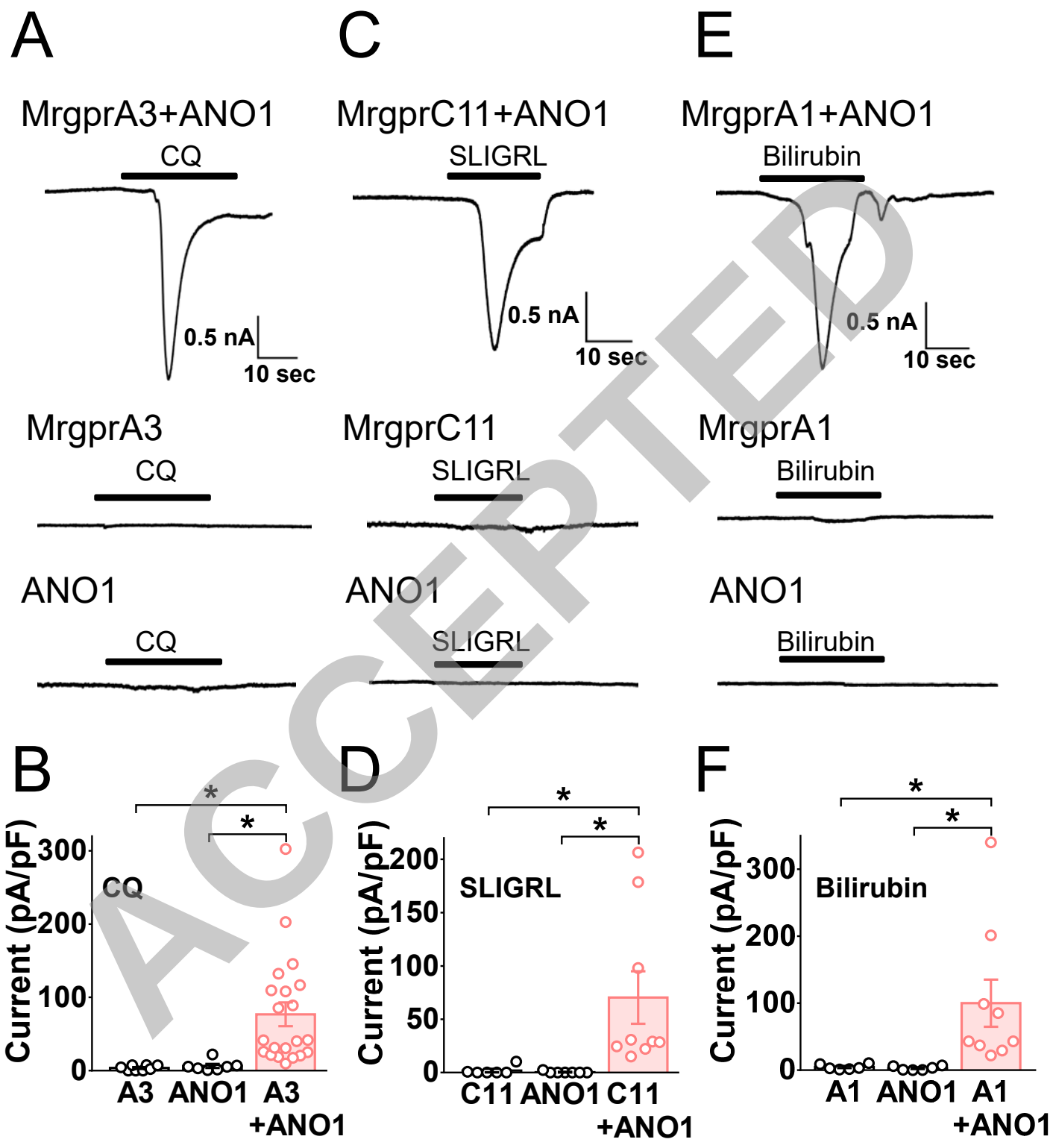

Figure 6

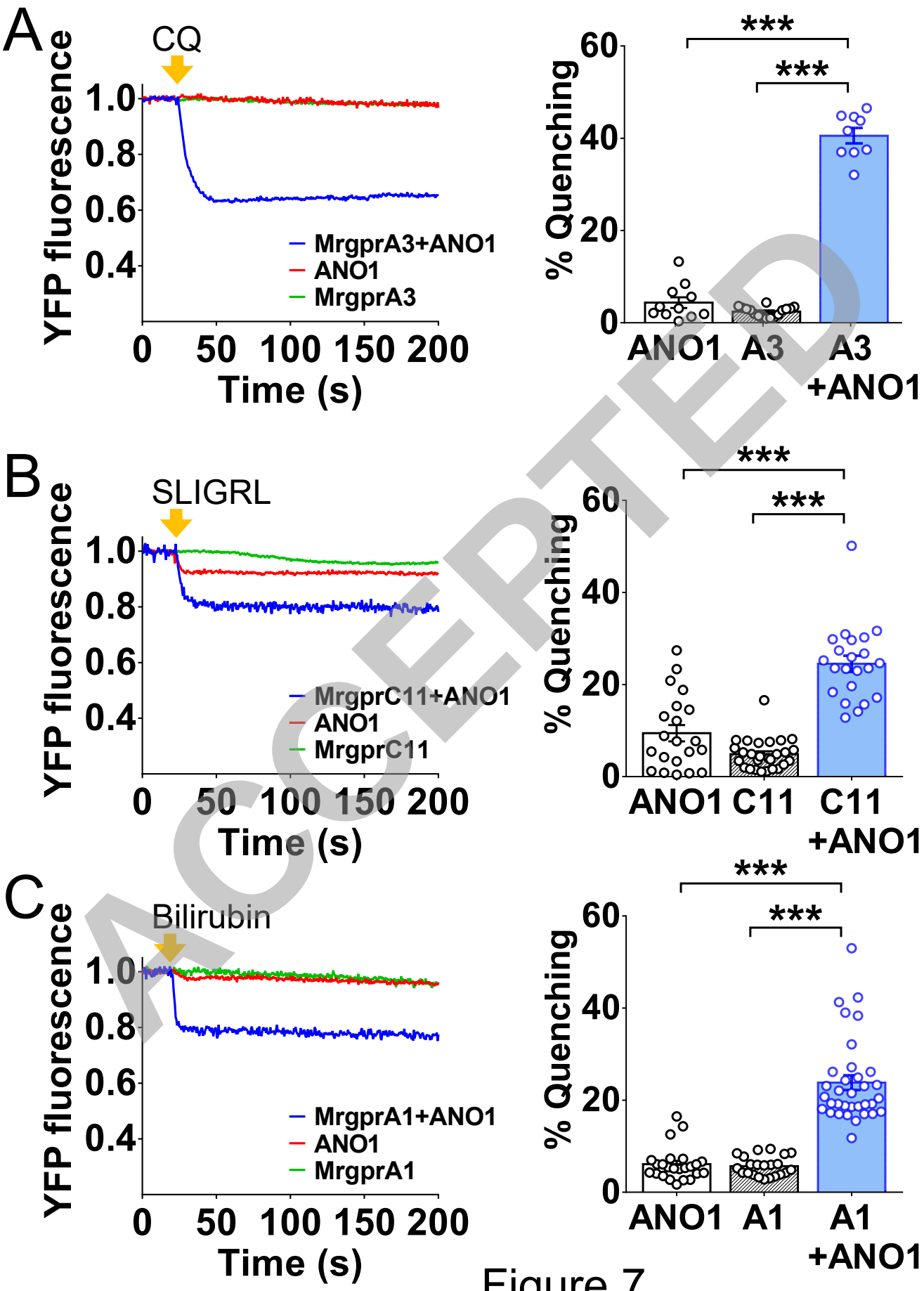

Figure 7

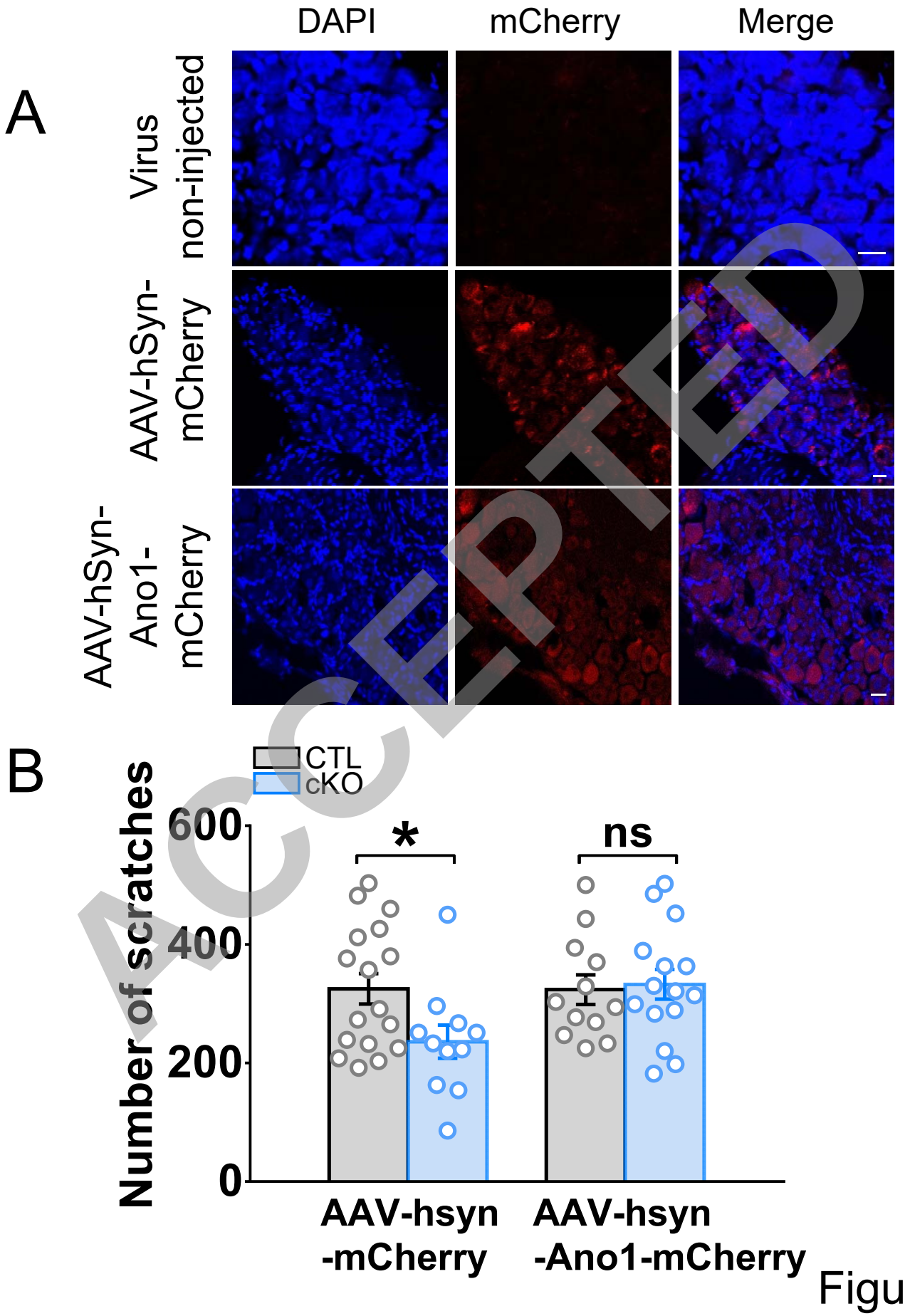

Figure 8